PAIR-PARTICLE DISPERSION IN TWO DIMENSIONAL SPH

D.D. Meringolo[1], S. Servidio[2], C. Meringolo[3], F. Aristodemo[4], P.G.F. Filianoti[1], P. Veltri[4], V. Carbone[2]
[1]Dipartimento D.I.C.E.A.M., Università Mediterranea di Reggio Calabria, 89124, Reggio Calabria, Italy.
[2]Dipartimento di Fisica, Università della Calabria, 87036, Arcavacata di Rende, Cosenza, Italy.
[3]Institut für Theoretische Physik, Max-von-Laue-Strasse 1, D-60438 Frankfurt, Germany.
[4]Dipartimento di Ingegneria Civile, Università della Calabria, 87036, Arcavacata di Rende, Cosenza, Italy.

I. Introduction

We revisit the classical fluid dynamics problem of pair-particle dispersion using the SPH model. Dispersion of fluid particles has relevant interest with regard to the understanding of the mechanisms of mass diffusion observed in turbulent flows. Investigations come back from the seminal paper presented in 1926 by Richardson [5], which proposed the well known $4/3$–law for the eddy diffusivity of pair particles advected by a turbulent high-Reynolds number flow. Here, we analyze the characteristic changes in the flow dynamics in terms of particles' dispersion behavior during the transition to turbulence. In the cases analyzed, focused on the laminar-turbulent transition, various scaling behaviors are observed. Specifically, these regard ballistic, super-diffusive, and diffusive dispersion regimes. These phases in the flow dynamics are identified and discussed. The problem is investigated in further detail by considering the probability density distributions of pair-particle distance separations in comparison with the theoretical expressions expected from Richardson's theory.

II. Pair-particle diffusive regimes

Richardson [5] observed that in turbulent flows the rate of pair diffusion, within a certain range, increases with the distance apart. Specifically, he considered the time evolution of the separation between two particles located at the initial time at coordinates $\boldsymbol{x}_1(t_0)$ and $\boldsymbol{x}_2(t_0)$. The mean value for the squared distance separation between those two particles $r = |\boldsymbol{r}_{12}| = |\boldsymbol{x}_1(t_0+\tau) - \boldsymbol{x}_2(t_0+\tau)|$, in turbulent fields at intermediate separations, is super-diffusive in time,

$$\langle r^2 \rangle \sim \tau^3. \tag{1}$$

Eq. (1) holds when the distance between the particles is of the same order of the dimension of the turbulent vortexes, corresponding to the inertial range of the energy cascade. The motion in the inertial range is very rapid, explosive in time, and related to the mixing properties of the turbulent field. As regards 2D turbulence, Babiano *et al.* [1] gave a theoretical background for the validity of Eq. (1) in the inertial range and proved it numerically, whereas experimental validation has been then provided by Jullien *et al.* [3].

A different kind of behavior is encountered when the particles are very close to each other, or in the condition of laminar flows,

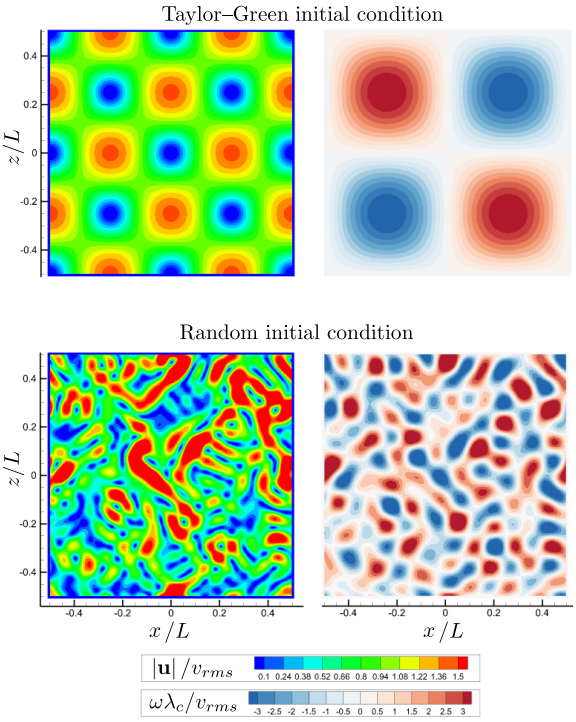

Fig. 1. Initial conditions: velocity (left) and vorticity (right) fields of the Taylor–Green vortex (top) and random condition (bottom).

in which case they conform to a ballistic transport (Batchelor [2]),

$$\langle r^2 \rangle \sim \tau^2. \tag{2}$$

For larger separation, *i.e.* when there is no more correlation between the particles' velocities, a different behavior is observed, which conforms to a Brownian motion. In that case, the classical law for the mean square displacement $\Delta \boldsymbol{s} = \boldsymbol{x}(t_0+\tau) - \boldsymbol{x}(t_0)$ is observed,

$$\langle \Delta s^2 \rangle = 2 D_s \tau, \tag{3}$$

with D_s the diffusion coefficient.

III. SPH simulations

Numerical simulations are performed through the δ-LES-SPH model (see *e.g.* [4]). The flow field is initialized by consider-

ing two different initial conditions: the classical Taylor–Green solution and a random initial condition, depicted in Fig. 1. In our campaign of simulations, four values of the Reynolds number are analyzed: $Re = 500$, 1000, 2500, and 10000. The Reynolds number is calculated at the initial time instant as $Re = v_{rms}\lambda_c/\nu$, in which v_{rms} is the root mean square velocity that, for our Lagrangian system of reference, can be defined as

$$v_{rms} = \sqrt{\frac{1}{N}\sum_{i=1}^{N} \boldsymbol{u}_i^2}, \tag{4}$$

with $\boldsymbol{u}_i$ the particle's velocity and N the overall number of fluid particles, λ_c the correlation length which, in a turbulent field, approximately corresponds to the size of the energy-containing eddies,

$$\lambda_c = \int C(r)\, dr, \tag{5}$$

where we assumed isotropy, and $C(r) = C(r_x, r_z)$ the two-points velocity autocorrelation function,

$$C(r_x, r_z) = \frac{1}{L^2}\int\int \boldsymbol{u}(x,z)\cdot\boldsymbol{u}(x+r_x, z+r_z)\, dx\, dz, \tag{6}$$

and ν the kinematic viscosity.

In the SPH simulations, the mean value of the separation is evaluated over all the couples of fluid particles that are horizontally distanced, at the beginning of the simulation, by the initial inter-particle distance, Δx, resulting in about 250000 pairs.

A. *Pair-particle dispersion*

In Fig. 2 the results for the Taylor–Green vortex initial condition are shown, in which we use $\tau = t\, v_{rms}/\lambda_c$. In all the cases, the flow dynamics very rapidly conform to a ballistic transport. For the case $Re = 500$, the dynamic is essentially ballistic for the whole duration, while only for values of $t\, v_{rms}/\lambda_c > 34$ a slope higher than 2 is observed. This may be the footprint of the inception of a super-diffusive behavior even in the most viscous case. In the cases $Re = 1000$, 2500, and 10000, the transition to a super-diffusive behavior is clearly observable at approximately $t\, v_{rms}/\lambda_c \simeq 28$, 25, and 18, respectively. In these cases, the averaged squared pair separation clearly follows the turbulent scaling.

The mean pair-particles separation value as a function of time for the random initial condition is shown in Fig. 3 for the four values of analyzed Reynolds number. Also in this case, ballistic and super-diffusive behaviors are clearly observable. Compared to the previous case, the τ^3 law appears early in the simulation even at the lowest Reynolds number. Specifically, the transition from ballistic to turbulence scaling occurs smoothly in the time window $t\, v_{rms}/\lambda_c \in [1, 3]$, for all the Reynolds numbers, which corresponds to a time instant one order of magnitude earlier than that of the Taylor–Green vortex. The earlier triggering of turbulence is due to the faster timescales and smaller correlation lengths. This is evident even at the lowest

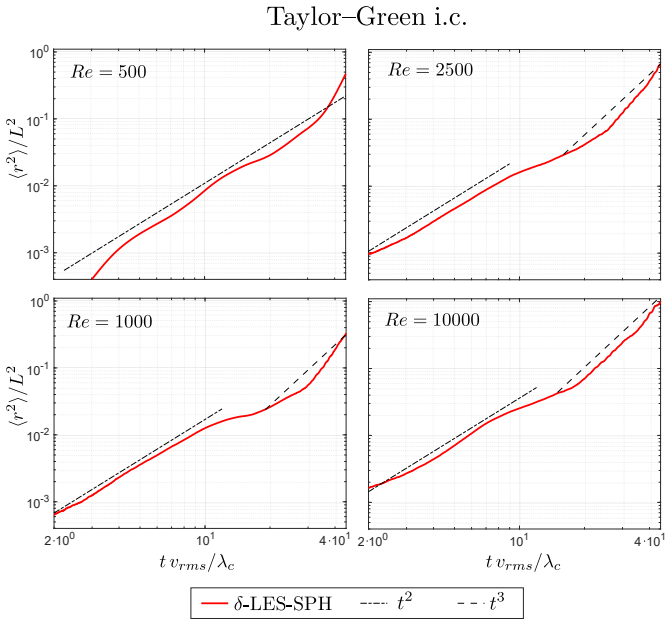

Fig. 2. Averaged squared pair separation for the Taylor–Green initial condition as a function of time for $Re = 500 - 10000$.

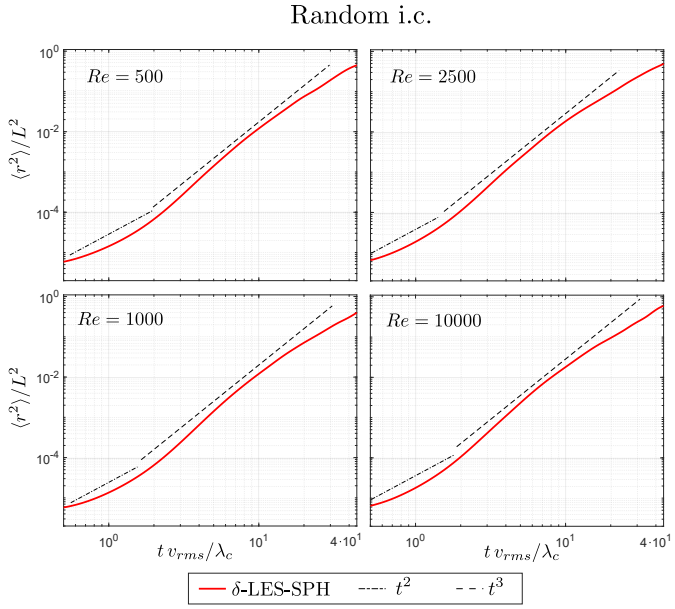

Fig. 3. Averaged squared pair separation for the random initial condition as a function of time for $Re = 500 - 10000$.

Reynolds number $Re = 500$ at $t\, v_{rms}/\lambda_c = 45$, in which the turbulent scaling is clearly observable. In this case, it is moreover possible to appreciate, for large times, the exhaustion of the turbulence scaling, with alleviation of the slope. This means that particle pairs are advected to distances in which underneath coherent structures are not present anymore in the turbulent field, resulting in the relaxation of the dispersion to a Brownian diffusion.

B. Probability density functions

Here we go into more detail, by analyzing the probability density distribution, $P(r,\tau)$, for two particles to be separated by a distance r at time τ. This analysis is inspired by the work of Richardson [5], which predicted that $P(r,\tau)$, for flows in turbulent conditions, obeys the following partial differential equation,

$$\frac{\partial P(r,\tau)}{\partial \tau} = \frac{1}{r}\frac{\partial}{\partial r}\left[r\chi(r)\frac{\partial P(r,\tau)}{\partial r}\right], \tag{7}$$

in which $\chi(r) = \chi_0 r^{2-\gamma}$ is a scale-dependent eddy diffusivity due to turbulence. In the case of homogeneous and isotropic turbulence, *i.e.* when the Kolmogorov's law is observed, $\gamma = 2/3$, so that the eddy-diffusivity scales as $\chi \sim r^{4/3}$. The solution to this equation, given as initial condition a Dirac delta distribution, $P(r,t_0) = \delta(r - r_0)$, and considering that $\int P(r,\tau)dr = 1$, is given by

$$\begin{aligned} P(r,\tau) &= \frac{A}{(\chi_0\gamma^2\tau)^{2/\gamma}}\exp\left(\frac{-r^\gamma}{\chi_0\gamma^2\tau}\right) \\ &= P_0(\tau)\exp\left(\frac{-r^\gamma}{\chi_0\gamma^2\tau}\right). \end{aligned} \tag{8}$$

This expression is valid for r sufficiently larger than r_0, corresponding to the inertial range length scales. In this analysis, the expression of $P(r,\tau)$ is calculated numerically by considering n classes, each of width Δr, such that the pair particles belonging to the i-th class are those for which $r \in [(i-1)\Delta r, i\Delta r]$. In our case, we set $\Delta r = 2\Delta x$. The probability of having two particles separated by distance r is thus evaluated by counting the number of pair particles falling into the corresponding class and dividing it by the total number of pair particles.

The initial pair-particle distribution in the simulations is thus given by $P(r,t_0) = \delta(r - \Delta x)$, being all the particle pairs equally spaced with the spatial resolution at $t = 0$. As the flow evolves in time the particles are progressively spread away from each other, thus the probability density function grows at large values of r and shrinks at small values of r. The probability density distribution expressed in Eq. (8) is adopted to fit the numerical simulations obtained for the cases $Re = 10000$. These results are shown, for different time instants, in Fig. 4 for both the Taylor–Green and random initial conditions. The fit is performed adopting $\gamma = 2/3$, as in Richardson's prediction. The fitting parameters are $\chi_0 = 0.0102$ and $P_0 = 0.0442$ for the Taylor–Green i.c., while $\chi_0 = 0.0101$ and $P_0 = 0.0461$ for the random i.c.

For large values of r, we can see that the Taylor–Green solution follows Richardson's prediction, while the random initial condition departs from it. In this case, these differences are related to the fact that in the random i.c. the vortical structures are smaller ($\lambda_c \simeq 0.048L$) than the Taylor–Green i.c. ($\lambda_c = 0.19L$), therefore at large distances the scaling of turbulence might be exhausted in the former case but not in the latter. On the other hand, the interesting difference that emerges from the obtained $P(r,\tau)$ is observed for small r in which the numerical result

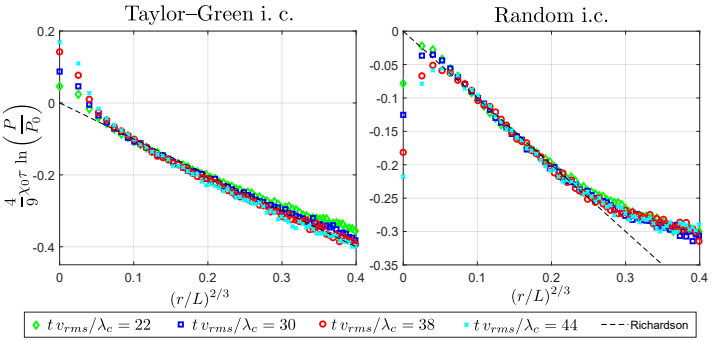

Fig. 4. Probability density functions of particles distance separation, $P(r,\tau)$, for the Taylor–Green (left) and Random (right) initial conditions, at different time instants for $Re = 10000$.

of the Taylor–Green i.c. overestimate Richardson's prediction, while the random i.c. underestimates it. This result might be related to some property of the initial conditions rather than the different dynamical evolution (earlier triggering of Richardson's scaling for the random i.c.), because at larger time instants the results tend to intensify their characteristic trends, rather than converge to the same behavior. Further analysis needs to be addressed to this issue.

IV. Conclusions

We investigated the time evolution of the statistics of pair-particles separations at different Reynolds numbers. For low Reynolds numbers the relative separation increases ballistically in time. As the Reynolds number increases, turbulence at small scales strongly pushes particles apart, so that the ballistic regime observed at short times for the relative separation, gives way to a super-ballistic Richardson's scaling at larger times. Such ballistic regime persists for a longer time in the Taylor–Green vortex i.c. compared with the random i.c., resulting in the latter to induce a transition to the Richardson's scaling at an earlier time in the simulations. The results obtained by the SPH simulations are in good agreement with the characteristics pair-particle dispersion laws observed during the transition from laminar to turbulent flow conditions.

Acknowledgment

This work has been financed by the National Recovery and Resilience Plan (NRRP), action EI TECH4YOU - SPOKE 1 Goal 3/PP 1AZ 2.

References

[1] Babiano, A., Basdevant, C., Le Roy, P., Sadourny, R.: Relative dispersion in two-dimensional turbulence. Jour. of Fluid Mech. **214**, 535–557 (1990)
[2] Batchelor, G.K.: Diffusion in a field of homogeneous turbulence: Ii. the relative motion of particles. In: Math. Proc. of the Cambridge Phil. Soc., vol. 48, pp. 345–362. Cambridge University Press (1952)
[3] Jullien, M.C., Paret, J., Tabeling, P.: Richardson pair dispersion in two-dimensional turbulence. Physical review letters **82**(14), 2872 (1999)
[4] Meringolo, D.D., Liu, Y., Wang, X.Y., Colagrossi, A.: Energy balance during generation, propagation and absorption of gravity waves through the δ-les-sph model. Coastal Engineering **140**, 355–370 (2018)
[5] Richardson, L.: Atmospheric diffusion shown on a distance-neighbour graph. Proc. of the Royal Soc. of London. **110**, 709–737 (1926)